Global biogenic isoprene emissions modulated by intensifying warm temperature extremes

Nyasulu, M., Rajasekar, A. ORCID: https://orcid.org/0000-0002-1917-0494, Yeboah, E. and Magara, G. (2026) Global biogenic isoprene emissions modulated by intensifying warm temperature extremes. Applied Geochemistry, 204. 106829. ISSN 1872-9134 doi: 10.1016/j.apgeochem.2026.106829 Available at https://centaur.reading.ac.uk/129680/

Applied Geochemistry 204 (2026) 106829

Contents lists available at ScienceDirect

Applied Geochemistry

journal homepage: www.elsevier.com/locate/apgeochem

Global biogenic isoprene emissions modulated by intensifying warm temperature extremes

Matthews Nyasulu [a], Adharsh Rajasekar [b,c,*], Emmanuel Yeboah [d], Genesis Magara [a]

[a] School of Ecology and Applied Meteorology, Nanjing University of Information Science and Technology, Nanjing, 210044, China
[b] Jiangsu Key Laboratory of Atmospheric Environment Monitoring and Pollution Control (AEMPC), Collaborative Innovation Centre of Atmospheric Environment and Equipment Technology (CIC-AEET), Nanjing University of Information Science &Technology, Nanjing, 210044, China
[c] School of Geography and Environmental Sciences, University of Reading, Reading, RG6 6AH, UK
[d] School of Remote Sensing and Geomatics Engineering, Nanjing University of Information Science and Technology, Nanjing, 210044, China

ARTICLE INFO

Editorial handling by Elisa Sacchi

Keywords:
Biogenic isoprene emissions
Climate feedback
Extreme temperature
Causal analysis

ABSTRACT

Biogenic isoprene, the most abundant non-methane volatile organic compound, plays a critical role in air quality and climate. While its emissions are known to be temperature-dependent, the specific causal link to the intensification of warm temperature extremes observed in recent decades remains understudied. This study provides causal evidence connecting the rising intensity of warm temperature extremes to trends in biogenic isoprene emissions from 2000 to 2019. We integrated high-resolution CAMS-GLOB-BIOv3.1 emission data with ERA5 reanalysis products and applied the Information Flow (IF) framework to quantify the causal influence of extreme temperature on isoprene emission trends. Our results reveal a significant increase in isoprene emissions (>1.2 Tg yr^{-1}) in tropical hotspots, which were significantly correlated with the intensity of extreme temperature ($r > 0.8$, $p < 0.05$). Importantly, causal analysis quantified a persistent, unidirectional IF from extreme temperatures to isoprene emissions, while the reverse pathway was negligible. This establishes extreme temperature as among the drivers of rising biogenic isoprene emissions, revealing a critical positive climate feedback loop under warming climate extremes. These findings highlight the need to incorporate extreme temperature–driven biogenic isoprene emission feedbacks into climate and air quality models to improve atmospheric composition and inform effective mitigation strategies for public health and climate stability.

1. Introduction

Isoprene strongly influences atmospheric composition, including ozone and fine particulate matter ($PM_{2.5}$), thereby affecting air quality and regional climate by altering Earth's atmospheric energy balance (Claeys et al., 2004; Unger, 2012). Isoprene is highly reactive, promoting tropospheric ozone formation under polluted conditions and contributing to the production of secondary organic aerosol (Claeys et al., 2004). A key oxidation product of isoprene is formaldehyde (CH_2O), which plays an important role in atmospheric photochemistry by shaping the oxidative capacity of the troposphere and serving as a major radical source that drives ozone formation (Millet et al., 2008). Owing to its short atmospheric lifetime and tight coupling to isoprene chemistry, formaldehyde is widely used as a proxy for isoprene emissions in satellite and ground-based observations (Palmer et al., 2006). On a global scale, isoprene emissions are overwhelmingly biogenic, with tropical forests representing the major source, temperate forests contributing moderate fluxes while agricultural and boreal ecosystems playing comparatively minor roles (Guenther et al., 2006; Harley et al., 2004).

Several approaches are used to study isoprene, including satellite observations (Palmer et al., 2006; Millet et al., 2008; Fu et al., 2019; Wells et al., 2020; Zhang and Gu, 2022), chemical transport and process-based models (Guenther et al., 2006; Pacifico et al., 2009; Unger, 2013; Monson et al., 2012; Cao et al., 2021), reanalysis products (Schwantes et al., 2020; Sindelarova et al., 2022), and ground-based measurements (Geron et al., 2000; Pacifico et al., 2009; Li et al., 2023). Among these, ground-based observations generally provide the most accurate, process-level constraints on emissions but are limited in spatial and temporal coverage. By contrast, satellites and models enable

* Corresponding author. Jiangsu Key Laboratory of Atmospheric Environment Monitoring and Pollution Control (AEMPC), Collaborative Innovation Centre of Atmospheric Environment and Equipment Technology (CIC-AEET), Nanjing University of Information Science &Technology, Nanjing, 210044, China.
E-mail address: a.rajasekar@reading.ac.uk (A. Rajasekar).

https://doi.org/10.1016/j.apgeochem.2026.106829
Received 3 November 2025; Received in revised form 5 April 2026; Accepted 13 April 2026
Available online 16 April 2026

analysis over longer periods and larger spatial domains, including the global scale, although with greater uncertainties than local in situ observations.

Isoprene emissions into the atmosphere depend strongly on environmental conditions, including temperature, ambient greenhouse-gas concentrations, and land-cover change (Singsaas and Sharkey, 2000; Arneth et al., 2007; Duncan et al., 2009; Heald et al., 2009; Stavrakou et al., 2014; Hantson et al., 2017; Chen et al., 2018; Zeng et al., 2023; DiMaria et al., 2025). For instance, a study by Singsaas and Sharkey. (2000) observed that isoprene emissions rise briefly when leaves are exposed to high temperatures (35–45 °C) and then decline to a regulated steady state in a reversible manner, demonstrating that temperature-induced reductions in isoprene above ~35 °C are driven by physiological control of isoprene synthesis rather than depletion, consistent with a protective role of isoprene against thermal stress. Isoprene emissions increase exponentially with temperature due to enhanced enzymatic activity, particularly of isoprene synthase, which catalyzes isoprene production in chloroplasts and exhibits strong temperature sensitivity (Monson et al., 1992; Oku et al., 2023). Arneth et al. (2007) also found that isoprene emissions typically increase under low CO_2 but decrease at elevated CO_2, and showed with a dynamic vegetation model that CO_2-driven inhibition of leaf isoprene production can offset warming- and productivity-induced increases, potentially moderating future ecosystem isoprene emissions and their atmospheric impacts. Furthermore, a recent study by Zeng et al. (2023) carried out over the Pearl River Delta, China, found that isoprene emissions from tropical and subtropical trees are strongly regulated by both temperature and light, and showed that the Guenther et al. (1993) algorithm accurately captures this dependence, confirming its suitability for simulating isoprene emissions in these ecosystems. In a recent study, Zeng et al. (2023) also found that isoprene emissions from tropical plants are more temperature-sensitive than those from temperate species under moderate conditions. However, during heatwaves, physiological stress lowers the optimum temperature, contrary to model predictions that assume acclimation based on long-term averages. This suggests that extreme heat may suppress isoprene emissions and that current models need revision to better capture these dynamics. In Arctic tundra, a study by Potosnak et al. (2013) showed that isoprene emissions can be significantly high under warm, bright conditions, affect atmospheric chemistry, and are expected to increase with climate warming. For mid-latitudes, Wang et al. (2024a,b) using the Model of Emissions of Gases and Aerosols from Nature (MEGAN) reported that sedges show a markedly stronger temperature response than other isoprene emitters predicted by widely used emission parameterizations. In the tropics, the apparent temperature dependence can also be modulated by confounding factors such as surface ozone and greenhouse gases (Duncan et al., 2009). These studies clearly demonstrate that multiple environmental factors influence isoprene emissions from vegetation into the atmosphere.

Despite extensive research on isoprene emissions and their environmental drivers, studies investigating how the recent rise in extreme temperature conditions influences these emissions remain limited, even though isoprene responds strongly to temperature changes (Guenther et al., 1995; Lathière et al., 2006). Recent work by Wang et al. (2024a,b) attributed long-term global isoprene emission trends to variations in CO_2 concentrations, vegetation dynamics, and meteorological factors using MEGANv3.2. However, that study primarily focused on decomposing overall emission trends into multiple drivers rather than isolating the specific role of extreme temperature intensity. Under extreme heat events, plant metabolic processes may be driven beyond their optimal physiological capacity, potentially triggering nonlinear increases in isoprene emissions that are not fully captured by analyses based solely on mean climate variability. In this study, we therefore examine the impact of recent intensifying warm extreme-temperature events on trends in isoprene emissions. We employ a statistical framework combining correlation analysis with a causality test to determine whether changes in the intensity of warm temperature extremes potentially drive the trends in isoprene emissions at the global scale. More details about the data and method used are given in Section 2, Section 3 presents the results, Section 5 interprets the results, while Section 4 summarises the conclusions drawn from the study.

2. Data and methods

2.1. CAMS emission inventories

This study used the high-resolution Copernicus Atmosphere Monitoring Service (CAMS) global biogenic inventory, CAMS-GLOB-BIO v3.1 (Sindelarova et al., 2022). CAMS-GLOB-BIO v3.1 estimates biogenic volatile organic compound (BVOC) emissions, including isoprene, monoterpenes, sesquiterpenes, methanol, acetone, and ethene, using the Model of Emissions of Gases and Aerosols from Nature (MEGAN v2.1) (Guenther et al., 2012). Isoprene emissions in CAMS-GLOB-BIO v3.1 are simulated by prescribed and static land-cover and plant functional type distributions, while responding dynamically to environmental and meteorological conditions. The simulation accounts for variability associated with air temperature, photosynthetically active radiation, leaf area index (LAI), soil moisture stress, leaf age phenology, and atmospheric CO_2 concentration. Specific BVOC emissions flux (F), such as isoprene, in MEGAN is calculated from a model grid cell as;

$$F = \gamma . EP . S \tag{1}$$

where γ is a dimensionless factor accounting for dependence of emissions on environmental factors such as air temperature, solar radiation, ambient CO_2 concentration, and LAI. EP is an emission potential defined under standardized environmental conditions, while S is a grid cell surface area (Sindelarova et al., 2022).

Based on Guenther et al. (2012), isoprene-temperature dependence during isoprene simulation is represented using a temperature activity factor, formulated as a weighted combination of light-dependent and light-independent emission components, reflecting contributions from both photosynthetic activity and stored carbon pools. The light-dependent component is described by an enzyme-kinetic function that captures the exponential increase in emissions with temperature up to an optimum, followed by a decline at higher temperatures due to enzymatic deactivation. Importantly, optimum is not constant but varies as a function of prior thermal conditions, increasing with the mean leaf temperature over the preceding 240 h to account for thermal acclimation. In addition, the emission capacity at the optimum temperature is scaled based on both short-term (24 h) and longer-term (240 h) temperature histories, thereby incorporating both immediate and acclimated physiological responses. Empirical coefficients further regulate the rate of temperature response and high-temperature inhibition, with values dependent on emission class, enabling a realistic representation of isoprene emission variability under changing thermal conditions. CAMS-GLOB-BIO v3.1 is built on the MEGANv2.1 framework and adopts the same isoprene–temperature dependence formulation for isoprene emissions.

Since land cover is prescribed in CAMS-GLOB-BIO v3.1, long-term variability and trends in simulated isoprene emissions primarily reflect changes in meteorological conditions and climate-driven vegetation activity rather than explicit land-use or deforestation changes, making the simulations suitable for assessing the influence of extreme temperature on biogenic isoprene emissions. The meteorological input for simulation is ERA5 reanalysis, by the European Center for Medium-Range Weather Forecasts (ECMWF) (Hersbach et al., 2020). The CAMS-GLOB-BIO v3.1 dataset spans from 2000 to 2019 and provides global coverage at 0.25° × 0.25° spatial resolution. Independent evaluations indicate that CAMS isoprene emissions are broadly consistent with other inventories, such as the European Monitoring and Evaluation Programme (EMEP) dataset (Sindelarova et al., 2022).

2.2. ERA5 reanalysis

We calculated extreme-temperature intensity using the fifth-generation ECMWF reanalysis (ERA5; Hersbach et al., 2020). ERA5 is produced with the Integrated Forecasting System (IFS) Cycle 41r2 (operational in 2016) and combines a global forecast model with diverse observations within a physically consistent data-assimilation framework. It provides hourly fields for the atmosphere, land, and ocean waves from 1940 to the present at 0.25° × 0.25° spatial resolution with near-real-time updates (~5-day latency) (Muñoz-Sabater et al., 2021). Because CAMS-GLOB-BIO v3.1 is driven by ERA5 meteorology to simulate BVOC emissions, including isoprene, using ERA5 to investigate extreme-temperature impacts ensures full consistency between the forcing data and the emission outputs. By leveraging ERA5, we maintain coherent meteorological drivers, accurately capture temperature extremes, and improve confidence that the observed correlations and causal links reflect true system behavior rather than artifacts of inconsistent forcing. In this study, we used daily maximum (2 m) air temperature to compute the intensity of warm temperature extremes and relate these metrics to biogenic isoprene emissions globally. Prior evaluations indicate that ERA5 reproduces temperature patterns and supports robust analysis of extreme-temperature events across diverse environments (Sheridan et al., 2020; Muñoz-Sabater et al., 2021; Velikou et al., 2022; Xu et al., 2022; Choudhury et al., 2023; Gbode et al., 2023; Erlat and Güler, 2024; Feron et al., 2024).

2.3. Calculation of warm extreme temperature intensity

The intensity of warm extreme temperature is calculated based on the definition by the Expert Team on Climate Change Detection and Indices (ETCCDI) framework (Alexander et al., 2006), a standardized suite of 27 core indices (16 temperature-based and 11 precipitation-based) widely used to monitor climate extremes. This study focused on the intensity of warm extreme temperature (TXx), defined as the annual maximum of daily maximum temperatures, mathematically expressed as;

$$TXx_y = \max\left(T_{max,1}, T_{max,2}.....T_{max,N}\right) \tag{2}$$

where $T_{max,1}, T_{max,2}.....T_{max,N}$ denotes the daily maximum temperature on days 1, 2 … N of the year y. The extreme-temperature index was calculated using R software. Many studies have applied ETCCDI indices to assess changes in temperature extremes across diverse regions, underscoring its robustness and comparability (Felix et al., 2021; Libanda, 2020; Wu and Huang, 2016; Xu et al., 2022; Felix et al., 2021; Kaushalya et al., 2025; Quenum et al., 2021; Wu and Huang, 2016; Yin and Sun, 2018).

2.4. Trend and correlation analysis

We used the Sen slope estimator (Sen, 1968) to quantify trend magnitude and the nonparametric Mann–Kendall (MK) test (Mann, 1945) to evaluate the significance of trends for both isoprene emission and TXx. These methods were chosen because they test for a monotonic trend against the null hypothesis of no trend without assuming a specific data distribution, and they perform better in the presence of missing values, outliers, and irregular sampling. Both Sen's slope and the MK test are widely applied to air quality and temperature time series (Cao et al., 2021; Almeida et al., 2017; Chathurangika et al., 2024; Nyasulu et al., 2023; Onyejuruwa et al., 2025; Shikwambana et al., 2020). Full computational details about the calculations can be accessed in the cited literature.

2.5. Correlation and causality test analysis

We examined the influence of extreme temperatures on isoprene emissions using Pearson's correlation and causality test analyses. Negative correlations were interpreted as evidence that higher warm-extreme temperature intensity suppresses isoprene emissions, whereas positive correlations indicate that the intensification of warm-extreme temperatures enhances emissions. To understand directionality beyond correlation, we applied the simplified information-flow framework to quantify the direct causal effect of extreme temperature on vegetation isoprene emissions. Rooted in stochastic dynamical systems theory, this method estimates the rate of information transfer between variables in a coupled time-series system (Liang, 2014; Hagan et al., 2019). Given a time series of intensity of warm temperature extremes as x and isoprene emissions as y, the causality of x on y is measured by the time rate of information flow from x to y, expressed as $T_{x\to y}$:

$$T_{x\to y} = \frac{1}{\delta_y^2}\left(\langle (dy)(x-\bar{x})\rangle - \frac{\delta_{xy}}{\delta_x^2}\langle (dx)(x-\bar{x})\rangle\right) \tag{3}$$

where δ_x^2 and δ_y^2 are the variances of x and y, respectively, and δ_{xy} is their covariance.

δ_x^2 and δ_y^2 are calculated as;

$$\delta_x^2 = \frac{1}{N}\sum_{t=1}^{N}(x_t-\bar{x})^2, \tag{4}$$

$$\delta_y^2 = \frac{1}{N}\sum_{t=1}^{N}(y_t-\bar{y})^2, \tag{5}$$

and δ_{xy} is expressed as;

$$\delta_{xy} = \frac{1}{N}\sum_{t=1}^{N}(x_t-\bar{x})(y_t-\bar{y}) \tag{6}$$

N is the number of points in time (t), while $\bar{x}$ and $\bar{y}$ are the temporal means of x and y, respectively. The information flow from y to x is calculated as the inverse of $T_{x\to y}$ $(T_{y\to y})$ from equation (3). We used cumulative causality estimates for a time series to reduce noise and capture long-term temporal changes. Positive IF values indicate that intensifying extreme temperatures have a positive impact on isoprene emissions; values near zero imply no detectable causal influence, while negative IF values indicate that rising temperatures suppress isoprene emissions.

3. Results and discussion

3.1. Annual and seasonal distribution of isoprene emissions

The annual distribution (Fig. 1) shows elevated isoprene emissions in the tropical and equatorial regions, particularly between ~30° S and 30°

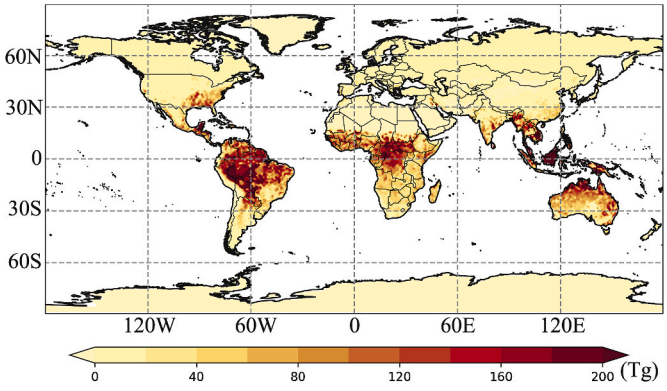

Fig. 1. Long-term annual spatial distribution of isoprene emissions based on the CAMS inventory during the 2000-2019 period.

N. Higher emissions occur over the Amazon Basin, Central Africa, and Southeast Asia, including Thailand, Indonesia, and northern Australia. These regions are generally dominated by dense vegetation, including tropical forests (Pegoraro et al., 2004), resulting in high biogenic isoprene emissions. These hotspot regions provide an ideal natural environment to investigate the dependence of isoprene emissions on high temperatures and solar radiation, which stimulate biogenic release (Arneth et al., 2008, 2011). Elevated emissions are also evident over the Southeastern United States of America (USA), consistent with prior USA-focused analyses (Opacka et al., 2021; Geddes et al., 2022). Relatively low isoprene emissions are detected in most mid-to high-latitude regions, indicating a lower emission potential of isoprene from vegetation compared to most tropical and equatorial regions. Seasonally (Fig. 2), there is pronounced seasonal variability that reflects shifts in vegetation and temperature activity. During DJF (December–February), elevated emissions appear across South America, Central and Southern Africa, Australia, Indonesia, and parts of India. In MAM (March–May), emissions weaken over much of the Southern Hemisphere (South America, Southern Africa, Australia) and shift northward, with notably higher emissions detected in Central Africa extending into West Africa, the Amazon, and Indonesia. High isoprene emissions are also observed over the southeastern USA. By JJA (June–August), emissions decline over Central Africa and Australia while remain comparatively high over the Amazon. High isoprene is detected in the tropical regions of the Northern Hemisphere, especially in the southeastern USA and southeastern China, consistent with prior satellite-based assessments (Millet et al., 2008).

The pattern reverses during SON (September–November), when biogenic isoprene emissions shift southwards and are concentrated along the tropics of the Southern Hemisphere, notably northern Australia, South America, and Southern Africa. It can be noted from the above seasonal pattern that isoprene emissions show a seasonal pattern corresponding to temperature changes, with high isoprene emissions during summer (hot) seasons in all hemispheres. During the summer season, such as the JJA season in the Northern Hemisphere, higher temperatures and increased rainfall stimulate vegetation growth, resulting in high isoprene emissions, as seen in the Southeastern USA and Southeastern China (Fig. 2) (Piao et al., 2019; Opacka et al., 2021; Lou et al., 2023). The opposite pattern occurs during DJF in the Southern Hemisphere summer, yielding elevated isoprene emissions. The observed summer peaks of isoprene emissions in both hemispheres underscore the coupled influence of biospheric processes and meteorological drivers, particularly temperature, radiation, and moisture content (Guenther et al., 2012; Sindelarova et al., 2014).

3.2. *Trends of isoprene and its relationship with the intensity of extreme temperature*

The spatial trends in Fig. 3 revealed widespread increases in biogenic isoprene emissions, with high magnitudes of positive trends detected across most tropical and equatorial regions, including Southeastern USA, the Amazon Basin, Central and Southern Africa, Northern Australia, Thailand, and the Indonesian Archipelago. It can also be observed that the largest magnitudes occur in regions that already exhibit high annual and seasonal totals (Figs. 1 and 2), implying that established hotspots are intensifying their contributions to atmospheric isoprene.

Localized negative trends are also evident, which might have been influenced by regional variability in meteorological conditions and ecosystem stress, including water stress and drought, which can suppress biogenic emissions (Li et al., 2025; Pegoraro et al., 2004; Trimmel et al., 2023). Such factors may reduce vegetation activity and emission capacity on seasonal to interannual time scales, leading to localized decreases in isoprene emissions, however, the observed negative trends were generally statistically non-significant (Fig. 3). The rising isoprene emissions have substantial implications for air quality and climate, as elevated isoprene enhances the formation of tropospheric ozone and secondary organic aerosols (SOAs), hence degrading air quality and harming human health (Lee et al., 2014; Wei et al., 2024; Khan et al., 2025). In addition, the high magnitude of trends along the tropics suggests an association between biogenic isoprene emissions, temperature, and vegetation activity, implying a potential positive climate–biosphere

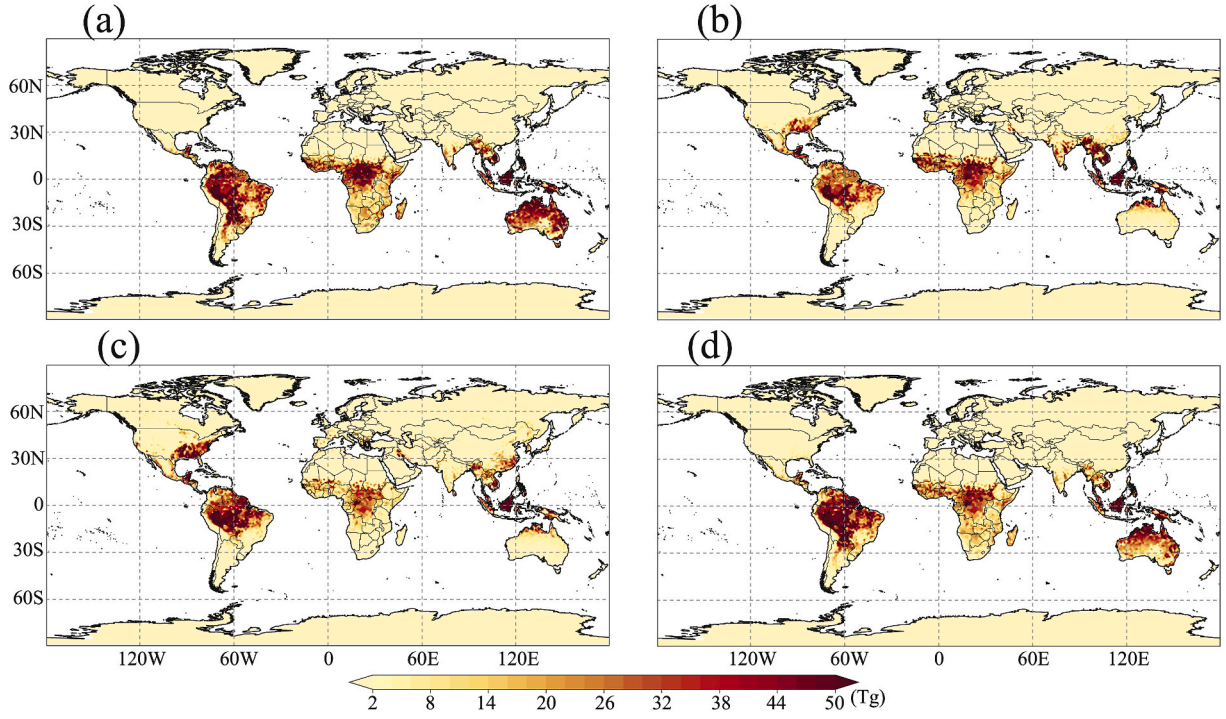

Fig. 2. Seasonal distribution of isoprene emissions for DJF (a), MAM (b), JJA (c), and SON (d). The distributions are calculated as the seasonal mean during the 2000-2019 period.

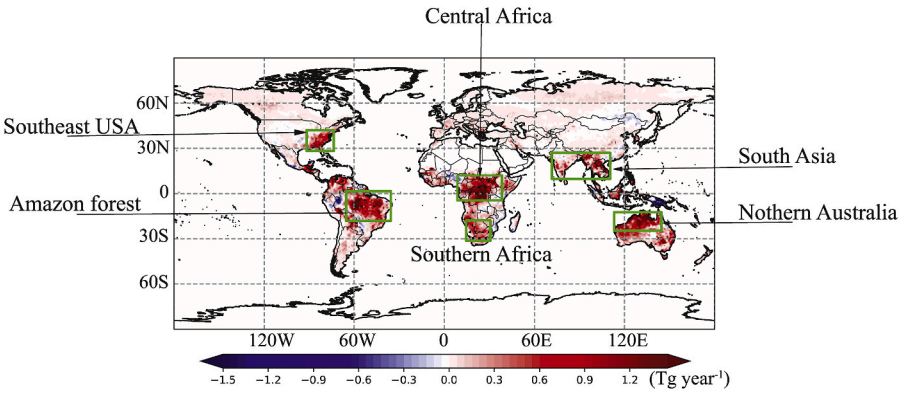

Fig. 3. Spatial distribution of isoprene emission trends from 2000 to 2019. The green rectangles indicate regions with high magnitudes of positive trends, selected for analysis of temporal variations. (For interpretation of the references to colour in this figure legend, the reader is referred to the Web version of this article.)

feedback, whereby persistent high temperature conditions stimulate additional isoprene emissions, unlike in mid and high latitudes regions where temperature contrast is very high (Pacifico et al., 2009).

To understand the influence of TXx on isoprene emissions, we analyzed trends of TXx globally and compared them with trends in biogenic isoprene emissions. Results in Fig. 4 show a dominant, widespread positive signal of TXx across most of the globe, indicating a general intensification of extreme temperatures.

The strongest increase is observed across the northern mid and high latitudes, including Alaska, Europe, and Siberia, where TXx is spatially extensive and statistically significant ($p < 0.05$). Positive trends in TXx are also evident in most parts of Southern America, Africa, and Australia, with significant trends over Northern and Southern Africa, the Amazon basin, and most of Australia. Intensification of extreme temperature conditions in most parts of the globe has also been documented in several recent studies (Almeida et al., 2017; Collins, 2022; Da Silva et al., 2019). In contrast, localized areas of weak or negative trends occur in parts of the Northern USA, extending into eastern Canada and southern Greenland. Isolated parts of the South Asia and Antarctica region also revealed negative trends; however, they are generally weaker than the dominant positive trends.

The spatial correlation between TXx and isoprene emissions exhibits pronounced regional contrasts shaped by both thermal regimes and vegetation distribution. To ensure statistical robustness and physical interpretation, correlation analysis was restricted to regions with detectable biogenic isoprene emissions, thereby avoiding dilution of the biospheric signal by areas devoid of vegetation, such as deserts. Results in Fig. 5 revealed significant positive correlations between TXx and isoprene emissions, which dominate in most parts of the globe, signifying a strong association between changes in TXx and isoprene

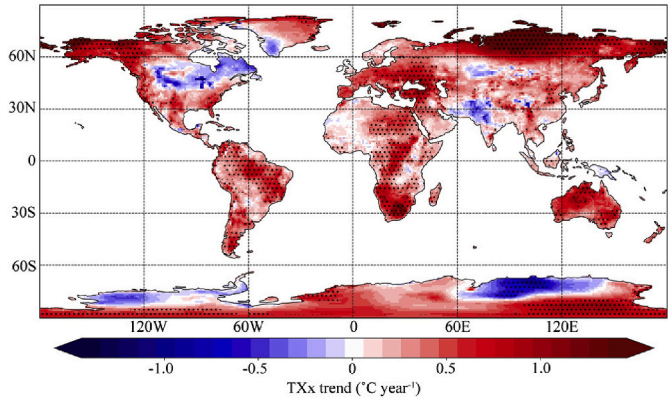

Fig. 4. Spatial distribution of TXx trends from 2000 to 2019. Hatched regions (.) indicate trends are significant at 95% confidence level ($p < 0.05$).

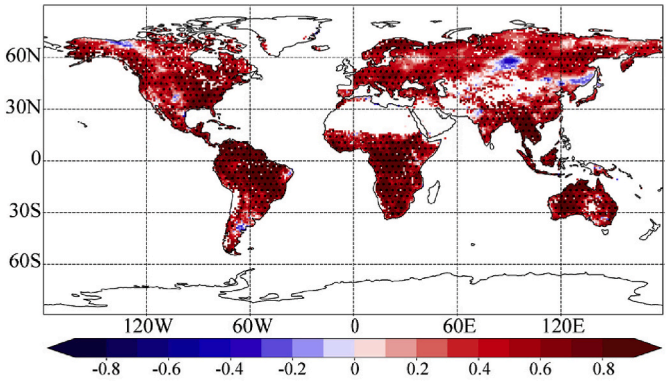

Fig. 5. Spatial distribution of correlation between isoprene emission and the intensity of extreme temperature during the study period. Black dots indicate regions where the correlation is significant at the 95% confidence level.

emissions. In tropical forest regions such as the Amazon, Central Africa, and Southeast Asia, correlations between TXx and isoprene emissions are typically strong ($r > 0.8$, $p < 0.05$), indicating that warm extreme temperatures strongly modulate emission variability in ecosystems characterized by dense vegetation and high biogenic activity. A significant correlation between isoprene and TXx is also evident in most parts of Europe, the Siberian region, and Alaska, indicating a strong association between isoprene emissions and extreme temperature intensity. Although correlations between TXx and isoprene emissions are strong and significant in mid to high-latitude regions, the magnitude of absolute trends remain relatively lower than in the tropics (Fig. 3). This indicates that while isoprene can strongly respond to wam extreme temperature conditions, the overall magnitude of isoprene emission is constrained by other regional factors such as vegetation density, vegetation type, length of growing season and water stress, which influences variation in trends across different parts of the globe (Pegoraro et al., 2004; Grote et al., 2013). It can, however, be noted that in some isolated locations, such as the West of the Amazon forest, West Africa, and Northeast China, isoprene trends are negative (Fig. 3) while temperature trends are positive (Fig. 4).

In addition, we compared trends in isoprene emissions with changed in mean temperature to distinguish the influence of mean temperature from that of extreme temperature intensity. The results (Fig. S1) indicate that the spatial pattern of mean temperature trends is broadly consistent with that of extreme temperature intensity across much of the globe. Significant positive trends are observed over Europe, Alaska, the Siberian region, and the Southeastern United States. Similarly, positive mean temperature trends align with TXx trends over the Amazon forest, as well as Central, Southern, and Northeastern Africa, and Australia,

whereas negative trends are evident in eastern Canada, parts of North America, Greenland, and South Asia. The consistency in trend patterns between mean temperature and TXx indicates that they covary, which is important for understanding whether isoprene is influenced more by TXx or mean temperature, particularly in equatorial and tropical regions. Correlation analysis (Fig. S2) also reveals the strongest relationships in tropical and equatorial regions, including the Amazon forest, Central and Southern Africa, Australia, South Asia, and much of the Southeastern United States. In contrast, weaker correlations are observed in mid-to high-latitude regions, particularly over Europe and Russia, where correlations are generally insignificant, ranging from weakly negative to weakly positive across Eastern Europe and Russia. A significant positive correlation is notable, however, in isolated locations. Comparison between isoprene-mean temperature correlation (Fig. S2) and isoprene-TXx correlation (Fig. 5) shows that mid to high latitude regions, such as over Europe and Russia, exhibit significant positive correlations between isoprene and TXx as compared to isoprene and mean temperature, indicating a stronger sensitivity of isoprene emissions to extreme temperature intensity than to mean temperature. These results suggest that while mean and extreme temperatures exert similar influence in tropical regions, their effects diverge in mid-to high latitudes, where isoprene emissions respond more strongly to extremes. Further analysis based on controlled simulations is necessary to isolate the influence of extreme temperatures from that of mean temperatures, specifically in tropical regions where their trends covary.

We further examined coevolution over time between isoprene emissions and TXx in regions that exhibited high magnitudes of positive trends in isoprene emissions from Fig. 3 using standardized anomalies (deviations from each variable's mean). It can be noted from Fig. 6 that interannual fluctuations in isoprene emissions closely matched those of extreme temperatures. Correlations are strong and statistically significant ($r > 0.7$, $p < 0.05$), indicating a high association between isoprene emission trends and the intensity of extreme temperatures in the regions. In addition, a close interannual alignment between isoprene emissions and TXx across all selected regions (Fig. 6) indicates that extreme temperature variability strongly modulates year-to-year emission changes. The pronounced correlations across tropical and subtropical regions reflect the strong temperature sensitivity of isoprene production in densely vegetated ecosystems. This demonstrates that extreme temperature intensification alone is sufficient to enhance biogenic emission fluxes, highlighting a climate-driven feedback mechanism independent of land-use change.

Further analysis of the isoprene emission-TXx response using linear and exponential models (Fig. 7) revealed both linear and nonlinear

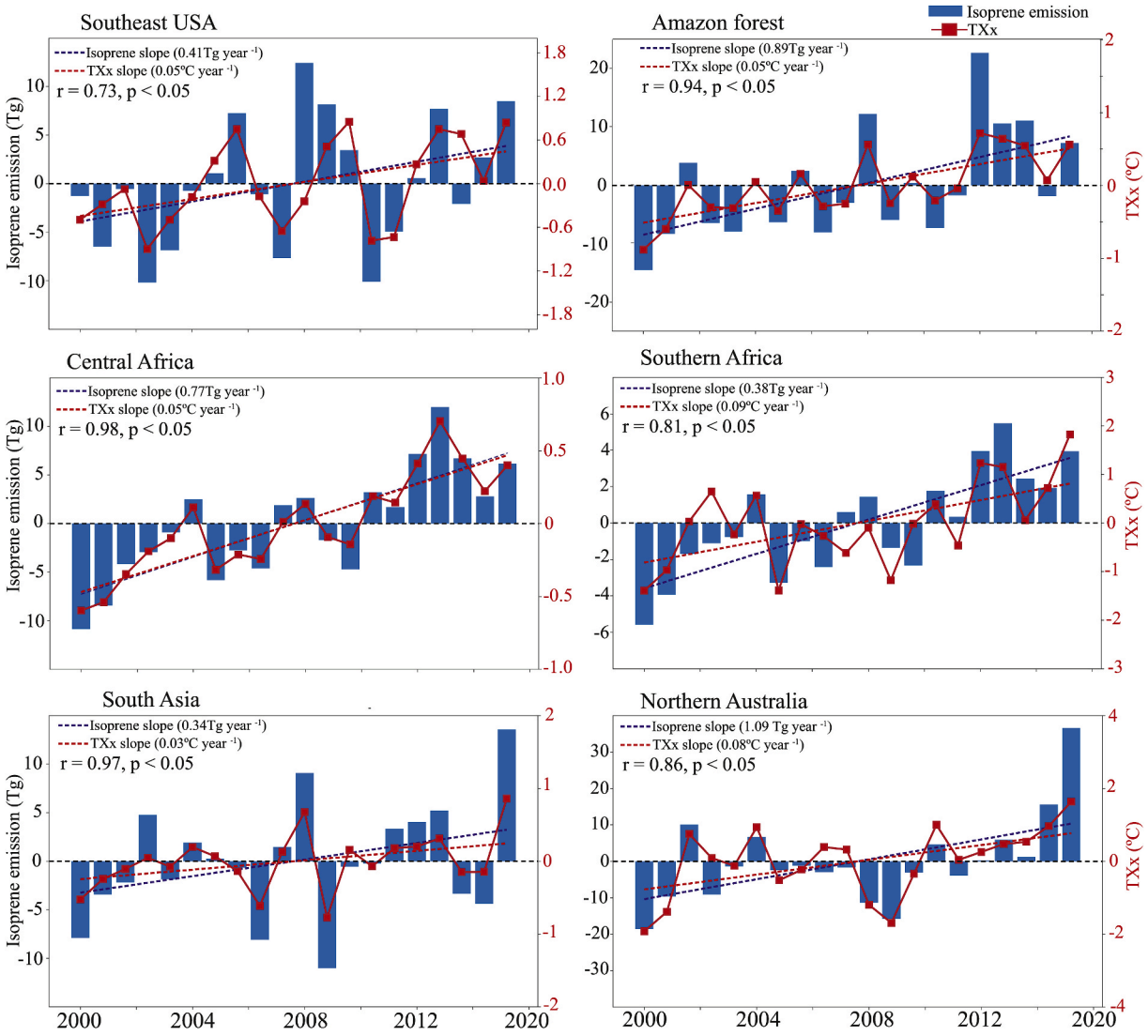

Fig. 6. Temporal distribution of isoprene emission anomalies and the intensity of extreme temperature over the selected regions. Regions with high trend magnitudes were selected for analysis (indicated by green polygons in Fig. 3). (For interpretation of the references to colour in this figure legend, the reader is referred to the Web version of this article.)

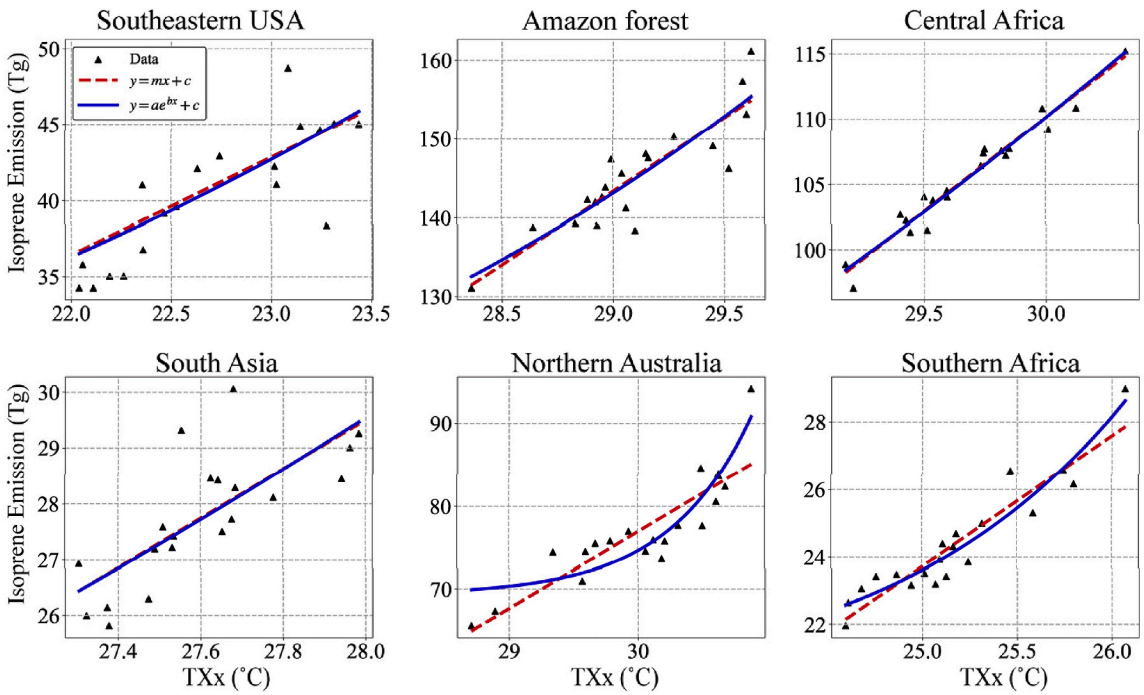

Fig. 7. Scatter plots showing the relationship between isoprene emissions and intensity of extreme temperature (TXx). The graph lines represent linear (red dashed) and exponential (blue) responses of isoprene to changes in TXx. (For interpretation of the references to colour in this figure legend, the reader is referred to the Web version of this article.)

positive responses; however, their strengths and forms vary regionally. As shown in Fig. 7, in the southeastern USA, Amazon forest, Central Africa, and South Asia, the temperature–isoprene response is predominantly linear, as indicated by the close alignment between linear and exponential fits, suggesting a linear response of emissions to extreme warming. In contrast, Northern Australia and Southern Africa exhibit a pronounced exponential response, with emissions increasing more rapidly at higher extreme temperatures, indicating strong nonlinear amplification of isoprene emissions under such conditions. These findings, however, differ from studies conducted at short temporal and leaf-area scales, where the isoprene-temperature response is exponential and diminishes at high temperatures (Rasulov et al., 2010). The linear-to-exponential response indicates the combined influence of thermal acclimation in MEGANv2.1 (Guenther et al., 2012), temporal aggregation, and background warming. Thermal acclimation shifts the optimum temperature to higher values under warmer conditions, allowing isoprene emissions to remain elevated even at high temperatures, while temporal aggregation at the annual scale smooths out short-term declines associated with extreme heat. Findings from this study imply that regions with extreme warming may disproportionately enhance biogenic isoprene emissions. These dynamics carry important implications for atmospheric chemistry, as isoprene is a key precursor of tropospheric ozone and SOAs (EPA, 2021). Consequently, continued intensification of extreme heat events may amplify tropical isoprene emissions, perturb regional oxidant balances, and exacerbate air pollution episodes.

3.3. Causal test analysis

Unlike correlation, which only measures the strength and direction of statistical association, and in regions where year-to-year co-variability dominates, positive correlations can emerge even when long-term trends differ. Causality tests evaluate whether changes in one variable drive changes in another over time (Liang, 2014; Hagan et al., 2019). Here, we applied a causal analysis to test whether intensifying warm extreme-temperature events increase biogenic isoprene emissions in regions with strong positive emission trends. This approach is well-suited to isolate dominant drivers, given that isoprene responds to multiple influences, including vegetation type, drought, temperature, and greenhouse gases (Guenther et al., 2006; Pacifico et al., 2009). As shown in Fig. 8, IF estimates from extreme temperatures to isoprene emissions increase consistently across all analyzed locations, with the Amazon, Central Africa, and South Asia showing the strongest signals. These results indicate that rising isoprene emissions are not merely coincident with warming but are significantly driven by the intensification of temperature extremes. A downward IF is notable over the Southeastern USA during 2004–2006; however, it remains positive, suggesting other factors, such as drought stress, may have strongly modulated isoprene emission. For instance, Wang et al. (2022) demonstrated that drought stress can substantially suppress biogenic isoprene emissions over the Southeastern USA, and that incorporating drought effects into emission modeling improves agreement with observed atmospheric chemistry during dry periods, highlighting that isoprene fluxes are modulated not only by temperature changes but also by moisture stress. The results from this study over the Southeastern USA coincide with the drought observed during 2004-2007 (Seager et al., 2009; Manuel, 2008). This demonstrates that other factors can influence the causal impact of extreme temperature on isoprene emissions.

Across tropical regions, including the Amazon, Central Africa, and South Asia, IF values were consistently high, indicating a strong causal influence of intensifying extreme temperatures on enhanced isoprene emissions. By contrast, the reverse pathway (IF from isoprene to extreme temperature) is near zero in all regions, implying that although isoprene responds strongly to temperature extremes, it does not directly drive extreme-temperature events at local to regional scales. Because tropical ecosystems account for most global isoprene emissions, the strong causal link between temperature and isoprene indicates that continued extreme warming will elevate isoprene emissions. This increase is likely to enhance ozone formation and secondary aerosol formation, thereby affecting regional radiative forcing and air-quality dynamics (Pacifico et al., 2012).

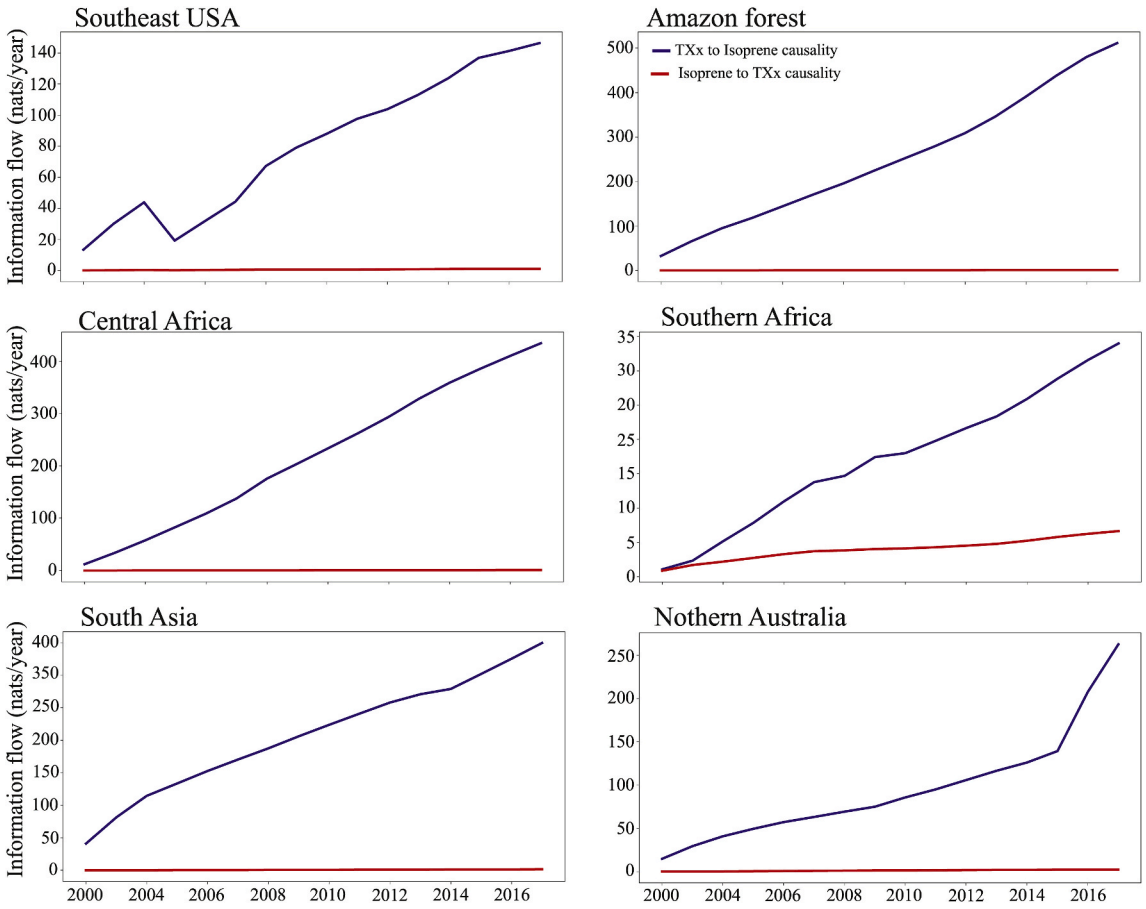

Fig. 8. Temporal distribution of information flow between isoprene emissions and the intensity of extreme temperatures over the selected regions with high magnitudes of spatial trends, as shown in Fig. 3. The blue line represents the information flow from extreme temperature to isoprene. In contrast, the red graph represents the information flow from isoprene to extreme temperature. (For interpretation of the references to colour in this figure legend, the reader is referred to the Web version of this article.)

4. Discussion

This study provides a global-scale analysis of isoprene emissions and establishes a causal relationship between the intensification of extreme temperatures and trends in biogenic isoprene emissions. The combined spatial, temporal, and causal evidence offers a more comprehensive understanding of biosphere–atmosphere feedback under extreme temperature conditions. The seasonal pattern detected in the present study, where isoprene emission is high in the Southern Hemisphere during summer (DJF) and in the Northern Hemisphere during summer (JJA), corresponds to seasonal changes in temperature and thus provides a stronger foundation for understanding the impact of extreme temperature conditions on isoprene emissions. Regions with strong DJF emissions, such as Southern Africa and Northern Australia, transition to weaker signals in JJA as temperatures and vegetation decrease, while peak emissions shift northward into the Northern Hemisphere. Biogenic isoprene emissions peak when vegetation density and temperatures are highest because emissions are directly linked to photosynthetic activity, leaf area, and temperature-dependent enzymatic production in chloroplasts (Guenther et al., 2006). Additionally, isoprene functions as a protective compound against thermal and oxidative stress, enhancing emissions under warm conditions (Monson et al., 2021; Rodrigues et al., 2023). Trend analyses at an annual scale have revealed a general positive trend of isoprene with high magnitude of positive trends detected in regions with high levels of isoprene emissions, specifically in the tropics and equatorial regions (Fig. 3). This implies that regions with already high isoprene levels are experiencing accelerated levels of isoprene, hence worsening pollution levels associated with biogenic emissions.

Correlation analysis between isoprene emissions and extreme-temperature intensity demonstrates that increasing heat extremes influence isoprene trends across much of the globe, consistent with previous studies (Stavrakou et al., 2014; Chen et al., 2018), showing enhanced isoprene emissions under warming conditions. These results suggest a positive climate–biosphere feedback, whereby warming extremes elevate BVOC emissions, potentially affecting air quality and radiative forcing (Pacifico et al., 2009). A comparison between the correlation patterns (Fig. 5) and emission trends (Fig. 3) highlights the distinction between thermal sensitivity and absolute emission magnitude. Tropical and equatorial forest regions, such as the Amazon, Central Africa, Southeast Asia, and Northern Australia, exhibit strong temperature sensitivity and high baseline emission capacity, leading to strong correlations and large positive trends in isoprene emissions. In contrast, some parts of Europe, Russia, and North America, such as Alaska, exhibit similarly strong correlations, indicating high responsiveness to extreme temperature changes; however, the magnitude of long-term trends is relatively low. The low magnitude of isoprene emission trends in some parts of mid to high latitude regions despite a significant correlation with extreme temperature as compared to tropical regions is because of high baseline emission potential in tropical regions, which are generally associated with variation vegetation type, LAI and water stress between these regions (Guenther et al., 1993; Potosnak et al., 2013; Chen et al., 2018). Importantly, land cover is prescribed in the present analysis; the spatial variability in correlation and trend magnitude reflects the interplay between factors such as vegetation type and climatic constraints, including temperature and moisture availability. High-emitting vegetation, such as broadleaf deciduous forests, dominates the tropical

response, while low-emitting land cover types, such as crops, grasses, and urban surfaces, contribute little, even under extreme heat (Sindelarova et al., 2014). In mid-latitudes, some species, such as sedges, show relatively strong extreme-temperature responses (Wang et al., 2024a,b), which explains part of the observed variability in Europe and North America in the present study (Fig. 4).

By comparing the response of isoprene emissions to mean and extreme temperatures, we find smaller differences in tropical and equatorial regions. In contrast, mid-to high-latitude regions exhibit larger differences, with isoprene responding more strongly to extreme temperatures. This is because tropical ecosystems operate under persistently high baseline temperatures that are already close to the biochemical optimum for isoprene production (Sharkey and Monson, 2017), resulting in similarly strong sensitivities to both incremental changes in mean temperature and extreme temperature conditions. In addition, tropical vegetation exhibits high temperature sensitivity (Guenther et al., 2006) but may experience physiological constraints such as heat stress or down-regulation during extreme temperature events, which can limit further enhancement beyond the mean temperature response (Zeng et al., 2023). In addition, most studies at short-time and leaf-level, isoprene emission increases non-linearly, generally exponentially with temperature up to an optimum range (~35–40 °C), reflecting the kinetics of isoprene synthase and the supply of photosynthetic precursors (Guenther et al., 2012; Sharkey and Monson, 2017; EPA, 2021). Beyond this optimum, physiological and enzymatic constraints may limit emissions. These previous findings differ from the present results at the long-term and annual scales. The linear-to-exponential response observed in the present results reflects the combined effects of thermal acclimation in MEGANv2.1 (Guenther et al., 2012), temporal aggregation, and background warming. Thermal acclimation increases the optimum temperature under warmer conditions, enabling isoprene emissions to remain high even at elevated temperatures (Guenther et al., 2012; Monson et al., 1992; Rasulov et al., 2015), while temporal aggregation at the annual scale averages out short-term reductions associated with extreme heat. Other studies using field observations (Vettikkat et al., 2023) have also demonstrated that isoprene emissions increase substantially under anomalously high temperatures. The observed linear-to-exponential increase in isoprene emissions implies that, in the long term, extreme warming may substantially enhance the availability of natural precursors for ozone and secondary organic aerosol formation, thereby degrading air quality. This response suggests that air quality risks could intensify disproportionately during extreme heat events, even in regions with limited anthropogenic emissions. The IF analysis strengthens this interpretation, in which a positive increase in IF from extreme temperatures to isoprene indicates that warming extremes are not merely coincident with higher fluxes but exert a directional influence on emission variability. At the same time, the magnitude and pattern of the response depend on ecosystem structure. Recent studies have further highlighted that vegetation-driven BVOC emissions, such as isoprene, can significantly influence urban atmospheric chemistry, and that species composition and regional chemical regimes determine whether greening strategies improve or worsen air quality (Mircea et al., 2023; Maison et al., 2024). Thus, under a warming climate characterized by intensifying heat extremes, vegetation–atmosphere interactions may amplify ozone and aerosol formation unless urban and regional land-management policies account for BVOC emission potential.

The demonstrated causal linkage between intensifying extreme temperatures and increasing biogenic isoprene emissions in the present study also implies that climate change–driven temperature extreme warming can amplify natural contributions to atmospheric pollution through biosphere–atmosphere feedback. Therefore, future air quality health risks may rise even without additional increases in anthropogenic emissions, but under natural conditions during extreme warming. Consequently, climate mitigation efforts aimed at limiting the frequency and intensity of extreme temperature events can also help reduce pollution associated with temperature-sensitive BVOCs. Incorporating temperature-driven biogenic emission responses into air quality management and climate adaptation strategies is therefore essential, particularly in tropical and densely vegetated areas where both heat extremes and emission potentials are increasing rapidly.

5. Conclusions

This study has demonstrated that the intensification of extreme temperatures significantly influences the trends of biogenic isoprene emissions. By leveraging two decades of high-resolution data and robust causal analysis, we extend the analysis beyond mere correlation to establish a definitive, unidirectional link between extreme heat and enhanced biogenic output. Our findings confirm that major tropical ecosystems, including the Amazon, Central Africa, and South Asia, are not only emission hotspots but also regions experiencing the most rapid acceleration in isoprene emissions, tightly coupled to the rising intensity of warmer extreme temperatures.

The causal relationship, quantified through Information Flow analysis, provides mechanistic clarity to observed global trends and underscores a significant positive climate-biosphere feedback. As climate warming accelerates, more frequent and intense heat extremes are likely to amplify vegetation's response, increasing the release of isoprene, a key precursor to tropospheric ozone and SOAs. The response of isoprene emissions to extreme temperatures has direct implications for the intensification of regional air pollution episodes and introduces complex perturbations to the atmospheric energy balance. Consequently, mitigating the factors that drive extreme temperature conditions may help reduce pollution levels associated with isoprene emissions.

The major limitation of this study is that the analyses rely on statistical comparisons, which may make it difficult to isolate the main driving factors in environments where variables covary, such as trends in mean and extreme temperatures. Controlled model simulations of long-term isoprene emissions under mean and extreme temperature conditions are therefore necessary to complement the present findings. Model products, despite broad validation, retain uncertainties in vegetation representation, emission factors, and extreme-temperature estimates, particularly in sparsely observed regions, and may hence influence the results. In addition, the annual-scale analysis captures robust signals but omits seasonal variability and moisture–heat interactions that may influence isoprene responses. Hence, further investigation into seasonal and sub-annual dynamics, including moisture–heat interactions, the number of summer days, and the length of the growing season, would capture variability not resolved at annual-scale analyses.

Funding

No funding was used in this study.

CRediT authorship contribution statement

Matthews Nyasulu: Conceptualization, Formal analysis, Methodology, Validation, Writing – original draft. **Adharsh Rajasekar:** Conceptualization, Data curation, Methodology, Supervision. **Emmanuel Yeboah:** Formal analysis, Writing – review & editing. **Genesis Magara:** Formal analysis, Visualization.

Declaration of competing interest

The authors declare that they have no known competing financial interests or personal relationships that could have appeared to influence the work reported in this paper.

Acknowledgements

The authors acknowledge editors and anonymous reviewers for their valuable and insightful comments.

Appendix A. Supplementary data

Supplementary data to this article can be found online at https://doi.org/10.1016/j.apgeochem.2026.106829.

Data availability

CAMS-GLOB-BIOv3.1 Biogenic isoprene emissions data: https://ads.atmosphere.copernicus.eu/datasets, ERA5 reanalysis (ECMWF) maximum temperature data: https://cds.climate.copernicus.eu/datasets.

References

Alexander, L.V., Zhang, X., Peterson, T.C., Caesar, J., Gleason, B., Klein Tank, A.M.G., et al., 2006. Global observed changes in daily climate extremes of temperature and precipitation. J. Geophys. Res. Atmos. 111 (5), 1–22. https://doi.org/10.1029/2005JD006290.

Almeida, C.T., Oliveira-Júnior, J.F., Delgado, R.C., Cubo, P., Ramos, M.C., 2017. Spatiotemporal rainfall and temperature trends throughout the Brazilian legal amazon, 1973–2013. Int. J. Climatol. 37 (4), 2013–2026. https://doi.org/10.1002/joc.4831.

Arneth, A., Monson, R.K., Schurgers, G., Niinemets, Ü., Palmer, P.I., 2008. Why are estimates of global terrestrial isoprene emissions so similar (and why is this not so for monoterpenes)? Atmos. Chem. Phys. 8 (16), 4605–4620. https://doi.org/10.5194/acp-8-4605-2008.

Arneth, A., Niinemets, Ü., Pressley, S., Bàck, J., Hari, P., Karl, T., et al., 2007. Process-based estimates of terrestrial ecosystem isoprene emissions: incorporating the effects of a direct CO2-isoprene interaction. Atmos. Chem. Phys. 7 (1), 31–53. https://doi.org/10.5194/acp-7-31-2007.

Arneth, A., Schurgers, G., Lathiere, J., Duhl, T., Beerling, D.J., Hewitt, C.N., et al., 2011. Global terrestrial isoprene emission models: sensitivity to variability in climate and vegetation. Atmos. Chem. Phys. 11 (15), 8037–8052. https://doi.org/10.5194/acp-11-8037-2011.

Cao, S., Zhang, S., Gao, C., Yan, Y., Bao, J., Su, L., et al., 2021. A long-term analysis of atmospheric black carbon MERRA-2 concentration over China during 1980–2019. Atmos. Environ. 264 (April), 118662. https://doi.org/10.1016/j.atmosenv.2021.118662.

Chathurangika, N.P.M., Haque, M., Nyasulu, M., Khan, R., Ahmed, F., Jui, J.F., et al., 2024. Long-Term Observation of Black Carbon and Its Relationship with Aerosol Radiative Forcing over South Asia Related Articles that may Interest you Forcing over South Asia, vol. 38, pp. 1105–1121. https://doi.org/10.1007/s13351-024-4046-5, 6.

Chen, W.H., Guenther, A.B., Wang, X.M., Chen, Y.H., Gu, D.S., Chang, M., et al., 2018. Regional to global biogenic isoprene emission responses to changes in vegetation from 2000 to 2015. J. Geophys. Res. Atmos. 123 (7), 3757–3771. https://doi.org/10.1002/2017JD027934.

Choudhury, D, Ji, F, Nishant, N, Di Virgilio, G, 2023. Evaluation of ERA5-Simulated Temperature and Its Extremes for Australia. Atmosphere 14 (6), 913. https://doi.org/10.3390/atmos140609.

Claeys, M., Graham, B., Vas, G., Wang, W., Vermeylen, R., Pashynska, V., et al., 2004. Formation of secondary organic aerosols through photooxidation of isoprene. Science 303 (5661), 1173–1176. https://doi.org/10.1126/science.1092805.

Collins, B., 2022. Frequency of compound hot–dry weather extremes has significantly increased in Australia since 1889. J. Agron. Crop Sci. 208 (6), 941–955. https://doi.org/10.1111/jac.12545.

Da Silva, P.E., e Silva, C.M., Spyrides, M.H.C., Andrade, L., de, M.B., 2019. Precipitation and air temperature extremes in the Amazon and northeast Brazil. Int. J. Climatol. 39 (2), 579–595. https://doi.org/10.1002/joc.5829.

DiMaria, C.A., Jones, D.B.A., Ferracci, V., Bloom, A.A., Worden, H.M., Seco, R., et al., 2025. Optimizing the temperature sensitivity of the isoprene emission model MEGAN in different ecosystems using a metropolis-hastings markov chain monte carlo method. J. Geophys. Res.: Biogeosciences 130 (5). https://doi.org/10.1029/2025JG008806 e2025JG008806.

Duncan, B.N., Yoshida, Y., Damon, M.R., Douglass, A.R., Witte, J.C., 2009. Temperature dependence of factors controlling isoprene emissions. Geophys. Res. Lett. 36 (5), 1–5. https://doi.org/10.1029/2008GL037090.

Erlat, E., Güler, H., 2024. Assessment of changes in absolute extreme temperatures in the Mediterranean region using ERA5-Land reanalysis data. Theor Appl Climatol 155, 9051–9066. https://doi.org/10.1007/s00704-024-05162-8.

Felix, M.L., Kim, Y.K., Choi, M., Kim, J.C., Do, X.K., Nguyen, T.H., Jung, K., 2021. Detailed trend analysis of extreme climate indices in the upper geum river basin. Water (Switzerland) 13 (22). https://doi.org/10.3390/w13223171.

Feron, S., Cordero, R.R., Damiani, A., et al., 2024. South America is becoming warmer, drier, and more flammable. Commun Earth Environ 5, 501. https://doi.org/10.1038/s43247-024-01654-7.

Fu, D., Millet, D.B., Wells, K.C., Payne, V.H., Yu, S., Guenther, A., Eldering, A., 2019. Direct retrieval of isoprene from satellite-based infrared measurements. Nat. Commun. 10 (1). https://doi.org/10.1038/s41467-019-11835-0.

Gbode, I.E., Babalola, T.E., Diro, G.T., et al., 2023. Assessment of ERA5 and ERA-Interim in Reproducing Mean and Extreme Climates over West Africa. Adv. Atmos. Sci. 40, 570–586. https://doi.org/10.1007/s00376-022-2161-8.

Geddes, J.A., Pusede, S.E., Wong, A.Y.H., 2022. Changes in the relative importance of biogenic isoprene and soil NOx emissions on ozone concentrations in nonattainment areas of the United States. J. Geophys. Res. Atmos. 127 (13). https://doi.org/10.1029/2021JD036361.

Geron, C., Guenther, A., Sharkey, T., Arnts, R.R., 2000. Temporal variability in basal isoprene emission factor. Tree Physiol. 20 (12), 799–805. https://doi.org/10.1093/treephys/20.12.799.

Grote, R., Monson, R.K., Niinemets, Ü., 2013. Leaf-level models of constitutive and stress-driven volatile organic compound emissions. In: Niinemets, Ü., Monson, R.K. (Eds.), Biology, Controls and Models of Tree Volatile Organic Compound Emissions. Springer Netherlands, Dordrecht, pp. 315–355. https://doi.org/10.1007/978-94-007-6606-8_12.

Guenther, A., Karl, T., Harley, P., Weidinmyer, C., Palmer, P.I., Geron, C., 2006. Estimates of global terrestrial isoprene emissions using MEGAN (Model of Emissions of Gases and Aerosols from Nature). Atmos. Chem. Phys. (6), 3181–3210.

Guenther, A.B., Jiang, X., Heald, C.L., Sakulyanontvittaya, T., Duhl, T., Emmons, L.K., Wang, X., 2012. The model of emissions of gases and aerosols from nature version 2.1 (MEGAN2.1): an extended and updated framework for modeling biogenic emissions. Geosci. Model Dev. (GMD) 5 (6), 1471–1492. https://doi.org/10.5194/gmd-5-1471-2012.

Guenther, A.B., Zimmerman, P.R., Harley, P.C., Monson, R.K., Fall, R., 1993. Isoprene and monoterpene emission rate variability: model evaluations and sensitivity analyses. J. Geophys. Res. Atmos. 98 (D7), 12609–12617. https://doi.org/10.1029/93JD00527.

Guenther, Alex, Nicholas, C., Fall, R., Klinger, L., Mckay, W.A., Scholes, B., 1995. A global model of natural volatile organic compound emissions s raja the balance triangle changes in the atmospheric accumulation rates of greenhouse triangle several inventories of natural and exposure assessment global scales have been two classes Fores. J. Geophys. Res. 100 (94), 8873–8892.

Hagan, D.F.T., Wang, G., Liang, X.S., Dolman, H.A.J., 2019. A time-varying causality formalism based on the liang-kleeman information flow for analyzing directed interactions in nonstationary climate systems. J. Clim. 32 (21), 7521–7537. https://doi.org/10.1175/JCLI-D-18-0881.1.

Hantson, S., Knorr, W., Schurgers, G., Pugh, T.A.M., Arneth, A., 2017. Global isoprene and monoterpene emissions under changing climate, vegetation, CO2 and land use. Atmos. Environ. 155, 35–45. https://doi.org/10.1016/j.atmosenv.2017.02.010.

Harley, P., Vasconcellos, P., Vierling, L., Pinheiro, C.C.D.S., Greenberg, J., Guenther, A., et al., 2004. Variation in potential for isoprene emissions among neotropical forest sites. Glob. Change Biol. 10 (5), 630–650. https://doi.org/10.1111/j.1529-8817.2003.00760.x.

Heald, C.L., Wilkinson, M.J., Monson, R.K., Alo, C.A., Wang, G., Guenther, A., 2009. Response of isoprene emission to ambient CO2 changes and implications for global budgets. Glob. Change Biol. 15 (5), 1127–1140. https://doi.org/10.1111/j.1365-2486.2008.01802.x.

Hersbach, H., Bell, B., Berrisford, P., Hirahara, S., Horányi, A., Muñoz-Sabater, J., et al., 2020. The ERA5 global reanalysis. Quart. J. Roy. Meteor. Soc. 146 (730), 1999–2049. https://doi.org/10.1002/qj.3803.

Kaushalya, K.C., Ampitiyawatta, A.D., Wimalasiri, E.M., Kumara, J.B.D.A.P., 2025. Annual and seasonal trends in extreme temperature events during 1981 to 2019 in dry zone, Sri Lanka. J. Agricult. Sci. - Sri Lanka. https://doi.org/10.4038/jas.v20i2.10475.

Khan, M.A.H., Holland, R., Mould, C., Bacak, A., Percival, C.J., Shallcross, D.E., 2025. Isoprene emissions, oxidation chemistry and environmental impacts. Atmosphere 16 (3), 1–32. https://doi.org/10.3390/atmos16030259.

Lathière, J., Hauglustaine, D.A., Friend, A.D., De Noblet-Ducoudré, N., Viovy, N., Folberth, G.A., 2006. Impact of climate variability and land use changes on global biogenic volatile organic compound emissions. Atmos. Chem. Phys. 6 (8), 2129–2146. https://doi.org/10.5194/acp-6-2129-2006.

Lee, K.-Y., Kwak, K.-H., Ryu, Y.-H., Lee, S.-H., Baik, J.-J., 2014. Impacts of biogenic isoprene emission on ozone air quality in the Seoul metropolitan area. Atmos. Environ. 96, 209–219. https://doi.org/10.1016/j.atmosenv.2014.07.036.

Li, Q., Gabay, M., Beznoshchenko, B., Fredj, E., Dayan, C., Tas, E., 2025. The effect of meteorological conditions during drought on BVOC mixing ratios over an eastern mediterranean forest. Sci. Total Environ. 1000, 180423. https://doi.org/10.1016/j.scitotenv.2025.180423.

Li, T., Baggesen, N., Seco, R., Rinnan, R., 2023. Seasonal and diel patterns of biogenic volatile organic compound fluxes in a subarctic tundra. Atmos. Environ. 292, 119430. https://doi.org/10.1016/j.atmosenv.2022.119430.

Liang, X.S., 2014. Unraveling the cause-effect relation between time series. Phys. Rev. E - Stat. Nonlinear Soft Matter Phys. 90 (5). https://doi.org/10.1103/PhysRevE.90.052150.

Libanda, B., 2020. Multi-model synthesis of future extreme temperature indices over Zambia. Model. Earth Syst. Environ. 6 (2), 743–757. https://doi.org/10.1007/s40808-020-00734-9.

Lou, C., Jiang, F., Tian, X., Zou, Q., Zheng, Y., Shen, Y., et al., 2023. Modeling the biogenic isoprene emission and its impact on ozone pollution in Zhejiang province,

China. Sci. Total Environ. 865 (December 2022), 161212. https://doi.org/10.1016/j.scitotenv.2022.161212.
Maison, A., Lugon, L., Park, S.-J., Baudic, A., Cantrell, C., Couvidat, F., et al., 2024. Significant impact of urban tree biogenic emissions on air quality estimated by a bottom-up inventory and chemistry transport modeling. Atmos. Chem. Phys. 24 (10), 6011–6046. https://doi.org/10.5194/acp-24-6011-2024.
Mann, H.B., 1945. Nonparametric tests against trend. Econometrica 13 (3), 245–259. https://doi.org/10.2307/1907187.
Manuel, J., 2008. Drought in the Southeast: Lessons for Water Management. Environmental Health Perspectives, United States. https://doi.org/10.1289/ehp.116-a168.
Millet, D.B., Jacob, D.J., Boersma, K.F., Fu, T.M., Kurosu, T.P., Chance, K., et al., 2008. Spatial distribution of isoprene emissions from North America derived from formaldehyde column measurements by the OMI satellite sensor. J. Geophys. Res. Atmos. 113 (2), 1–18. https://doi.org/10.1029/2007JD008950.
Mircea, M., Borge, R., Finardi, S., Briganti, G., Russo, F., de la Paz, D., et al., 2023. The role of vegetation on urban atmosphere of three European cities. Part 2: evaluation of vegetation impact on air pollutant concentrations and depositions. Forests 14 (6). https://doi.org/10.3390/f14061255.
Monson, R.K., Grote, R., Niinemets, Ü., Schnitzler, J.P., 2012. Modeling the isoprene emission rate from leaves. New Phytol. 195 (3), 541–559. https://doi.org/10.1111/j.1469-8137.2012.04204.x.
Monson, R.K., Jaeger, C.H., Adams, W.W., Driggers, E.M., Silver, G.M., Fall, R., 1992. Relationships among isoprene emission rate, photosynthesis, and isoprene synthase activity as influenced by temperature. Plant Physiol. 98 (3), 1175–1180. https://doi.org/10.1104/pp.98.3.1175.
Monson, R.K., Weraduwage, S.M., Rosenkranz, M., Schnitzler, J.-P., Sharkey, T.D., 2021. Leaf isoprene emission as a trait that mediates the growth-defense tradeoff in the face of climate stress. Oecologia 197 (4), 885–902. https://doi.org/10.1007/s00442-020-04813-7.
Muñoz-Sabater, J., Dutra, E., Agustí-Panareda, A., Albergel, C., Arduini, G., Balsamo, G., et al., 2021. ERA5-Land: a state-of-the-art global reanalysis dataset for land applications. Earth Syst. Sci. Data 13 (9), 4349–4383. https://doi.org/10.5194/essd-13-4349-2021.
Nyasulu, M., Gibson, F., Thulu, D., Alexander, F., 2023. An assessment of four decades atmospheric - PM 2 . 5 trends in urban locations over Southern Africa using MERRA - 2 reanalysis. Air Qual. Atmos. Health (3). https://doi.org/10.1007/s11869-023-01392-3.
Oku, H., Mutanda, I., Inafuku, M., 2023. Molecular characteristics of isoprene synthase and its control effects on isoprene emissions from tropical trees. J. Plant Res. 136 (1), 63–82. https://doi.org/10.1007/s10265-022-01418-4.
Onyejuruwa, A., Hu, Z., Towfiqul Islam, A.R.M., Nyasulu, M., Oo, K.T., 2025. Seasonal precipitation changes in response to long-term aerosol anomalies: a case from West Africa. Phys. Chem. Earth, Parts A/B/C 138, 103847. https://doi.org/10.1016/j.pce.2024.103847.
Opacka, B., Müller, J.F., Stavrakou, T., Bauwens, M., Sindelarova, K., Markova, J., Guenther, A.B., 2021. Global and regional impacts of land cover changes on isoprene emissions derived from spaceborne data and the MEGAN model. Atmos. Chem. Phys. 21 (11), 8413–8436. https://doi.org/10.5194/acp-21-8413-2021.
Pacifico, F., Folberth, G.A., Jones, C.D., Harrison, S.P., Collins, W.J., 2012. Sensitivity of biogenic isoprene emissions to past, present, and future environmental conditions and implications for atmospheric chemistry. J. Geophys. Res. Atmos. 117 (D22). https://doi.org/10.1029/2012JD018276.
Pacifico, F., Harrison, S.P., Jones, C.D., Sitch, S., 2009. Isoprene emissions and climate. Atmos. Environ. 43 (39), 6121–6135. https://doi.org/10.1016/j.atmosenv.2009.09.002.
Palmer, P.I., Abbot, D.S., Fu, T.M., Jacob, D.J., Chance, K., Kurosu, T.P., et al., 2006. Quantifying the seasonal and interannual variability of North American isoprene emissions using satellite observations of the formaldehyde column. J. Geophys. Res. Atmos. 111 (12), 1–14. https://doi.org/10.1029/2005JD006689.
Pegoraro, E., Rey, A., Greenberg, J., Harley, P., Grace, J., Malhi, Y., Guenther, A., 2004. Effect of drought on isoprene emission rates from leaves of Quercus virginiana Mill. Atmos. Environ. 38 (36), 6149–6156. https://doi.org/10.1016/j.atmosenv.2004.07.028.
Piao, S., Liu, Q., Chen, A., Janssens, I.A., Fu, Y., Dai, J., et al., 2019. Plant phenology and global climate change: current progresses and challenges. Glob. Change Biol. 25 (6), 1922–1940. https://doi.org/10.1111/gcb.14619.
Potosnak, M.J., Baker, B.M., Lestourgeon, L., Disher, S.M., Griffin, K.L., Bret-Harte, M.S., Starr, G., 2013. Isoprene emissions from a tundra ecosystem. Biogeosciences 10 (2), 871–889. https://doi.org/10.5194/bg-10-871-2013.
Quenum, G.M.L.D., Nkrumah, F., Klutse, N.A.B., Sylla, M.B., 2021. Spatiotemporal changes in temperature and precipitation in West Africa. Part i: analysis with the CMIP6 historical dataset. Water (Switzerland) 13 (24). https://doi.org/10.3390/w13243506.
Rasulov, B., Bichele, I., Hüve, K., Vislap, V., Niinemets, Ü., 2015. Acclimation of isoprene emission and photosynthesis to growth temperature in hybrid aspen: resolving structural and physiological controls. Plant Cell Environ. 38 (4), 751–766. https://doi.org/10.1111/pce.12435.
Rasulov, B., Hüve, K., Bichele, I., Laisk, A., Niinemets, Ü., 2010. Temperature response of isoprene emission in vivo reflects a combined effect of substrate limitations and isoprene synthase activity: a kinetic analysis. Plant Physiol. 154 (3), 1558–1570. https://doi.org/10.1104/pp.110.162081.
Rodrigues, J.S., Kovács, L., Lukeš, M., Höper, R., Steuer, R., Červený, J., et al., 2023. Characterizing isoprene production in Cyanobacteria – insights into the effects of light, temperature, and isoprene on Synechocystis sp. PCC 6803. Bioresour. Technol. 380, 129068. https://doi.org/10.1016/j.biortech.2023.129068.
Schwantes, R.H., Emmons, L.K., Orlando, J.J., Barth, M.C., Tyndall, G.S., Hall, S.R., et al., 2020. Comprehensive isoprene and terpene gas-phase chemistry improves simulated surface ozone in the southeastern US. Atmos. Chem. Phys. 20 (6), 3739–3776. https://doi.org/10.5194/acp-20-3739-2020.
Seager, R., Tzanova, A., Nakamura, J., 2009. Drought in the Southeastern United States: causes, variability over the last millennium, and the potential for future hydroclimate change. J. Clim. 22 (19), 5021–5045. https://doi.org/10.1175/2009JCLI2683.1.
Sen, P.K., 1968. Estimates of the regression coefficient based on Kendall's tau. J. Am. Stat. Assoc. 63 (324), 1379–1389. https://doi.org/10.1080/01621459.1968.10480934.
Sharkey, T.D., Monson, R.K., 2017. Isoprene research – 60 years later, the biology is still enigmatic. Plant, Cell \& Environment 40 (9), 1671–1678. https://doi.org/10.1111/pce.12930.
Sheridan, S.C., Lee, C.C., Smith, E.T., 2020. A comparison between station observations and reanalysis data in the identification of extreme temperature events. Geophysical Research Letters 47, e2020GL088120. https://doi.org/10.1029/2020GL08812.
Shikwambana, L., Mhangara, P., Mbatha, N., 2020. Trend analysis and first time observations of sulphur dioxide and nitrogen dioxide in South Africa using TROPOMI/Sentinel-5 P data. Int. J. Appl. Earth Obs. Geoinf. 91 (September), 102130. https://doi.org/10.1016/j.jag.2020.102130.
Sindelarova, K., Granier, C., Bouarar, I., Guenther, A., Tilmes, S., Stavrakou, T., et al., 2014. Global data set of biogenic VOC emissions calculated by the MEGAN model over the last 30 years. Atmospheric Chemistry and Physics 14 (17), 9317–9341. https://doi.org/10.5194/acp-14-9317-2014.
Sindelarova, Katerina, Markova, J., Simpson, D., Huszar, P., Karlicky, J., Darras, S., Granier, C., 2022. High-resolution biogenic global emission inventory for the time period 2000-2019 for air quality modelling. Earth System Science Data 14 (1), 251–270. https://doi.org/10.5194/essd-14-251-2022.
Singsaas, E.L., Sharkey, T.D., 2000. The effects of high temperature on isoprene synthesis in oak leaves. Plant, Cell and Environment 23 (7), 751–757. https://doi.org/10.1046/j.1365-3040.2000.00582.x.
Stavrakou, T., Müller, J.F., Bauwens, M., De Smedt, I., Van Roozendael, M., Guenther, A., et al., 2014. Isoprene emissions over Asia 1979-2012: impact of climate and land-use changes. Atmospheric Chemistry and Physics 14 (9), 4587–4605. https://doi.org/10.5194/acp-14-4587-2014.
Trimmel, H., Hamer, P., Mayer, M., Schreier, S.F., Weihs, P., Eitzinger, J., et al., 2023. The influence of vegetation drought stress on formaldehyde and ozone distributions over a central European city. Atmospheric Environment 304, 119768. https://doi.org/10.1016/j.atmosenv.2023.119768.
Unger, N., 2012. Global climate forcing by criteria air pollutants. Annual Review of Environment and Resources 37, 1–24. https://doi.org/10.1146/annurev-environ-082310-100824.
Unger, N., 2013. Isoprene emission variability through the twentieth century. Journal of Geophysical Research Atmospheres 118 (24). https://doi.org/10.1002/2013JD020978, 13,606-13,613.
Velikou, K, Lazoglou, G, Tolika, K, Anagnostopoulou, C, 2022. Reliability of the ERA5 in Replicating Mean and Extreme Temperatures across Europe. Water 14 (4), 543. https://doi.org/10.3390/w14040543.
Vettikkat, L., Miettinen, P., Buchholz, A., Rantala, P., Yu, H., Schallhart, S., et al., 2023. High emission rates and strong temperature response make boreal wetlands a large source of isoprene and terpenes. Atmospheric Chemistry and Physics 23 (4), 2683–2698. https://doi.org/10.5194/acp-23-2683-2023.
Wang, H., Liu, X., Wu, C., Lin, G., 2024a. Regional to global distributions, trends, and drivers of biogenic volatile organic compound emission from 2001 to 2020. Atmospheric Chemistry and Physics 24 (5), 3309–3328. https://doi.org/10.5194/acp-24-3309-2024.
Wang, H., Welch, A.M., Nagalingam, S., Leong, C., Czimczik, C.I., Tang, J., et al., 2024b. High temperature sensitivity of Arctic isoprene emissions explained by sedges. Nature Communications 15 (1). https://doi.org/10.1038/s41467-024-49960-0.
Wang, Y., Lin, N., Li, W., Guenther, A., Lam, J.C.Y., Tai, A.P.K., et al., 2022. Satellite-derived constraints on the effect of drought stress on biogenic isoprene emissions in the southeastern US. Atmospheric Chemistry and Physics 22 (21), 14189–14208. https://doi.org/10.5194/acp-22-14189-2022.
Wei, D., Cao, C., Karambelas, A., Mak, J., Reinmann, A., Commane, R., 2024. High-resolution modeling of summertime biogenic isoprene emissions in New York City. Environmental Science \& Technology 58 (31), 13783–13794. https://doi.org/10.1021/acs.est.4c00495.
Wells, K.C., Millet, D.B., Payne, V.H., Deventer, M.J., Bates, K.H., de Gouw, J.A., et al., 2020. Satellite isoprene retrievals constrain emissions and atmospheric oxidation. Nature 585 (7824), 225–233. https://doi.org/10.1038/s41586-020-2664-3.
Wu, C., Huang, G., 2016. Projection of climate extremes in the Zhujiang River basin using a regional climate model. International Journal of Climatology 36 (3), 1184–1196. https://doi.org/10.1002/joc.4412.
Xu, W., Lei, X., Chen, S., Yu, T., Hu, Z., Zhang, M., et al., 2022. How well does the ERA5 reanalysis capture the extreme climate events over China? Part II: extreme temperature. Frontiers in Environmental Science 10 (June), 1–15. https://doi.org/10.3389/fenvs.2022.921659.

Yin, H., Sun, Y., 2018. Characteristics of extreme temperature and precipitation in China in 2017 based on ETCCDI indices. Advances in Climate Change Research 9 (4), 218–226. https://doi.org/10.1016/j.accre.2019.01.001.

Zeng, J., Zhang, Y., Mu, Z., Weihua, P., Zhang, H., Wu, Z., et al., 2023. Temperature and light dependency of isoprene and monoterpene emissions from tropical and subtropical trees: field observations in south China. Applied Geochemistry 155, 105727. https://doi.org/10.1016/j.apgeochem.2023.105727.

Zhang, W., Gu, D., 2022. Geostationary satellite reveals increasing marine isoprene emissions in the center of the equatorial Pacific Ocean. Npj Climate and Atmospheric Science 5 (1), 1–9. https://doi.org/10.1038/s41612-022-00311-0.